

Research

The Results of Performance Measurements of Field-aged Crystalline Silicon Photovoltaic Modules

Artur Skoczek, Tony Sample^{*†} and Ewan D. Dunlop

DG-Joint Research Centre—Institute for Energy, Renewable Energy unit, Italy

This paper presents the results of electrical performance measurements of 204 crystalline silicon-wafer based photovoltaic modules following long-term continuous outdoor exposure. The modules comprise a set of 53 module types originating from 20 different producers, all of which were originally characterized at the European Solar Test Installation (ESTI), over the period 1982–1986. The modules represent diverse generations of PV technologies, different encapsulation and substrate materials. The modules electrical performance was determined according to the standards IEC 60891 and the IEC 60904 series, electrical insulation tests were performed according to the recent IEC 61215 edition 2. Many manufacturers currently give a double power warranty for their products, typically 90% of the initial maximum power after 10 years and 80% of the original maximum power after 25 years. Applying the same criteria (taking into account modules electrical performance only and assuming 2.5% measurement uncertainty of a testing lab) only 17.6% of modules failed (35 modules out of 204 tested). Remarkably even if we consider the initial warranty period i.e. 10% of P_{max} after 10 years, more than 65.7% of modules exposed for 20 years exceed this criteria. The definition of life time is a difficult task as there does not yet appear to be a fixed catastrophic failure point in module ageing but more of a gradual degradation. Therefore, if a system continues to produce energy which satisfies the user need it has not yet reached its end of life. If we consider this level arbitrarily to be the 80% of initial power then all indications from the measurements and observations made in this paper are that the useful lifetime of solar modules is not limited to the commonly assumed 20 year. Copyright © 2008 John Wiley & Sons, Ltd.

KEY WORDS: outdoor tests; qualification tests; long-term degradation

Received 23 September 2008

INTRODUCTION

Module lifetime is one of the crucial factors in determining the cost of solar electricity (together with the

system price, the annual solar irradiance, and the capital interest rate), which is why lifetime prediction related issues remain a topic of interest of many researchers. The effort to assure high reliability of photovoltaic modules has resulted in the introduction by the International Electrotechnical Commission (IEC) of accelerated test procedures termed “Module Design and Type Approval” the IEC 61215¹ and IEC 61215 edition 2.²

* Correspondence to: Tony Sample, DG-Joint Research Centre—Institute for Energy, Renewable Energy unit, Via E. Fermi 2749 Ispira, Varese 21027, Italy.

† E-mail: tony.sample@jrc.it

The IEC 61215 standard “lays down IEC requirements for the design qualification and type approval of terrestrial photovoltaic modules suitable for long-term operation in general open-air climates, . . .” The standard specifies its purpose as “. . .to determine the electrical and thermal characteristics of the module and to show, as far as is possible within reasonable constraints of cost and time, that the module is capable of withstanding prolonged exposure in climates described in the scope. The actual lifetime expectancy of modules so qualified will depend on their design, their environment, and the conditions under which they are operated. . .”

A failure according to the IEC 61215 is deemed to have occurred if the loss in maximum power following a test is greater than 5% + the repeatability of the power measurement of the control module. For a sequence of tests, failure occurs when the cumulative loss exceeds 8% + repeatability. The other failure modes are major visual defect (such as cracked cells, bubbles or delamination, or loss of mechanical integrity), open-circuit or ground faults detected during or after test execution, and finally electrical insulation failures.

The IEC 61215 helps manufacturers to assess module lifetime, against a minimum standard, but does not provide an unambiguous value of lifetime, which long-term field ageing can give. Long-term outdoor exposure in diversified climatic conditions intends to address all failure mechanisms which are difficult or impossible to simulate in the lab during time constrained accelerated tests.

Weathering is a continuous process but the magnitude of the effect will vary due to several factors. Sunlight has one of the greatest effects on outdoor weathering of PV modules and of this the majority of damage is caused by the ultraviolet component of the sunlight. The amount of sunlight is dependent on geographical location and altitude. Geographic location and positioning of the module has a significant effect on its weathering resistance. A module in a sunny environment will degrade faster due to increased UV content and elevated temperature. Exposure at elevated altitudes can significantly increase exposure to ultraviolet light and therefore significantly reduce the expected lifetime. Water, falling as rain or as atmospheric humidity, will also have an impact on the weathering resistance. Another factor is air pollution. Its sources may be natural, for example sea salt or dust, or man-made such as soot from exhaust fumes and industrial gases. Sulfur and other pollutants such as acidic fumes which can speed up the degradation

process stressing junction boxes, encapsulation material and cause not only the tarnishing of metal frames but also the front glass surface. Also module mounting system has an impact on modules aging. Roof mounted or building integrated modules usually run hotter than free rack-mounted ones.

DESCRIPTION OF THE EXPERIMENT

This paper presents the results of electrical performance measurements of 204 crystalline silicon wafer based photovoltaic modules (53 different module types) following long-term continuous outdoor exposure. Between 1983 and 1986 the European Solar Test Installation—ESTI laboratory installed (free rack-mounting) various sets of crystalline silicon wafer based photovoltaic modules at the ESTI outdoor field in the Ispra site. The climatic conditions of Ispra (located in northern Italy) at 220 m above sea level, where the weathering was executed, are considered to be a moderate subtropical climate (−10 to +35°C, with less than 90% RH). Before outdoor exposure most modules were tested at ESTI lab according to CEC501 test sequence,³ or individual parts of the sequence. The basic principles which were later used for the formation of the IEC 61215 were already applied in this standard, however, the test levels were notably less severe than are applied now.⁴ From the results of the application of the CEC501 none of these modules exhibited failure with regard to electrical performance (although two modules failed the electrical insulation test). These modules were then, on completion of the CEC501 tests, installed in the ESTI outdoor test site in racks allowing free circulation of air. One group of modules was connected to the grid inverter with the maximum power point tracking circuit, another group was connected to battery charger used occasionally for charging an electric car and finally the last group was mounted and left at the open circuit conditions. In the mid 1990s, all modules were disconnected and left in the open circuit conditions.

Before installation, all modules were characterized by measuring their electrical performance, visual inspection, and electrical insulation test.

The general measurement principle and equipment used in the 1980s and during the latest measurement campaign (2004) is very similar. Modules are measured utilizing the same Large Area Pulse Solar Simulator Spectrolab (LAPSS), which consists of two

Xenon pulse flash tube lamps at a distance of 13 m from the test plane. The electronic load has a voltage range of 1.0–100 V and a current range of 0.1–20 A. The shape of SpectroLab LAPSS pulse is trapezoidal with the flat part of the pulse at the set point of 1000 W/m² lasting for approximately 2 ms.

In the 1980s, the *I*–*V* curve data were recorded using dedicated equipment supplied by Spectrolab (8-bit, three channel data acquisition system). Later due to its failure, in the mid 1980s, the acquisition system was replaced by a 12-bit, four channel Krenz transient recorder and in the 2001 by the currently used Nicolet INTEGRA 20 digital oscilloscope with true 1 M sample/s sampling rate at 12-bit signal resolution. The module and the reference cell temperatures are measured with resistance temperature sensors PT-100.

The main changes introduced in the operation of the measurement system are the implementation of an improved STC temperature control $\pm 0.5^\circ\text{C}$ or better versus $\pm 2^\circ\text{C}$ in the 1980s and a new method of digital signal filtering and fitting of the maximum power point.

It should be noted that the reference cell utilized for the comparison of the modules electrical performance has been changed. The original reference cell R301 used 20 years ago was no longer available; hence all current measurements were performed with the reference cell PX202C. The calibration of the reference cells in the 1980s was much more difficult and the uncertainty of the calibration value of the R301 is not available. It was performed by the Royal Aircraft

Establishment (RAE) in Cyprus using an outdoor method. Since the idea of the experiment relies on relative measurements, utilization of a different reference cell can be questionable. In order to quantify the potential difference between the reference cells used for these measurements a series of modules which were measured in the 1980s and then kept under dark, dry storage conditions for the last 20 years have been re-measured using the new reference cell PX202C. It is assumed that the stored modules exhibited the same performance (especially modules I_{SC} since FF may be affected by interconnections degradation) in comparison to their initial state, although it is impossible to preclude their degradation. The results of these measurements are presented in the Table I.

The difference in measurements using the two reference cells is small. These results increase the confidence that any changes measured after long-term exposure are the result of aging and not due to change of reference cell.

CHARACTERISTICS OF THE MODULES

The main design details of all 53 different module types (204 individual pieces) are presented in Table II. The modules represent various commercially available silicon wafer based technology of the 1980s and incorporate different cell types, encapsulation, and substrate

Table I. Comparison of measurements performed with two reference cells: R301 in the 1980s and PX202C in 2008 on control modules stored in the dark

Polycrystalline modules												
Esti code	IC01			GA01			GC04			MA01		
Date	1986	2008	Δ [%]	1985	2008	Δ [%]	1987	2008	Δ [%]	1985	2008	Δ [%]
Voc [V]	22.30	22.16	–0.6%	20.83	20.89	0.30%	21.10	20.97	–0.63%	20.09	20.23	0.68%
FF [%]	71.00	69.91	–1.5%	75.60	75.38	–0.29%	72.80	72.64	–0.22%	75.20	75.23	0.04%
P_{MAX} [W]	37.10	35.63	–3.7%	43.39	43.07	–0.73%	44.90	44.35	–1.23%	35.95	35.89	–0.16%
I_{SC} [A]	2.34	2.30	–1.7%	2.75	2.73	–0.62%	2.91	2.91	0.07%	2.38	2.36	–0.87%
Monocrystalline modules												
Esti code	HH01			LE01			LE04			HO02		
Date	1987	2008	Δ [%]	1987	2008	Δ [%]	1988	2008	Δ [%]	1989	2008	Δ [%]
Voc [V]	21.71	21.32	–1.79%	21.62	21.39	–1.06%	21.66	21.27	–1.81%	21.20	21.14	–0.30%
FF [%]	69.72	69.41	–0.45%	76.01	76.29	–1.04%	75.50	75.09	–0.55%	70.90	71.01	0.16%
P_{MAX} [W]	41.47	40.75	–1.72%	48.77	47.54	–2.52%	47.90	46.99	–1.90%	43.00	42.37	–1.47%
I_{SC} [A]	2.74	2.75	0.52%	2.97	2.91	–2.02%	2.93	2.94	0.46%	2.86	2.82	–1.30%

Table II. Design details of investigated module series

Code (samples)	Cells	Strings	Cell type	Substrate material	Encapsulant	Total cell area [m ²]	Cell to module area ratio	Average module efficiency [%]	P_{MAX} [W]	Number of years outside
AC (6)	36	1	Mono	—	EVA	0.36	0.85	12.0	52	20
BA (2)	72	1	Mono	Silicone	Silicone	0.56	0.69	8.0	66	22
D0 (8)	72	1	Mono	Plastic	PVB	0.56	0.58	6.3	64	23
DA (2)	33	1	Poly	Tedlar, Al	PVB	0.33	0.75	8.5	37	22
E0 (2)	36	1	Mono	Glass	—	0.28	0.63	6.8	31	23
F0 (5)	20	1	Poly	Glass	PVB	0.20	0.78	7.1	18	23
FA (3)	40	1	Poly	Glass	PVB	0.40	0.81	9.1	40	23
FD (1)	40	1	Poly	Glass	PVB	0.20	0.78	7.4	19	23
FF (6)	40	1	Poly	Glass	PVB	0.40	0.81	7.9	39	20
H0 (4)	72	6	Mono	Silicone	Silicone	0.56	0.66	6.1	54	21
HA (6)	72	6	Mono	Silicone	Silicone	0.56	0.66	6.2	55	20
HB (2)	72	6	Poly	Tedlar	EVA	0.56	0.66	6.4	56	20
HD (4)	40	1	Poly	Tedlar	EVA	0.40	0.84	7.2	35	22
HE (4)	40	1	Poly	Glass	EVA	0.40	0.84	7.6	36	22
HF (2)	72	3	Mono	Tedlar	EVA	0.56	0.65	6.9	60	22
HG (2)	72	3	Poly	Tedlar	EVA	0.72	0.83	8.0	69	22
IA (8)	36	1	Mono	Glass	EVA	0.28	0.65	6.9	32	23
IB (2)	36	1	Mono	Glass	EVA	0.28	0.64	7.2	32	22
IC (6)	40	1	Poly	Glass	EVA	0.40	0.80	7.3	36	20
J0 (4)	36	3	Mono	Glass	Silicone	0.28	0.64	6.9	31	21
JA (8)	36	1	Poly	Glass	Silicone	0.36	0.79	6.9	31	21
JB (4)	36	1	Mono	Glass	EVA	0.36	0.81	10.5	47	20
L0 (2)	144	8	Mono	Polyester, Al	PVB	1.13	0.77	8.0	118	21
LA (8)	144	8	Mono	Polyester, Al	PVB	1.13	0.77	7.9	118	21
LB (8)	144	8	Mono	Polyester, Al	PVB	1.13	0.77	8.6	124	21
LD (2)	144	8	Mono	Polyester, Al	PVB	1.13	0.77	9.2	136	19
M0 (4)	80	4	Poly	Polyethylene	EVA	0.40	0.85	8.4	39	21
MA (6)	72	2	Poly	Tedlar, Al	EVA	0.33	0.88	9.6	36	21
N0 (4)	72	1	Mono	Plastic	PVB	0.56	0.58	7.1	68	23
NA (8)	36	1	Poly	Tedlar, Al	PVB	0.36	0.78	7.7	36	21
NB (2)	36	1	Poly	Glass	PVB	0.36	0.78	7.8	36	21
OA (4)	36	1	Mono	Tedlar, Al	EVA	0.28	0.64	7.4	33	21
OB (4)	36	1	Mono	Tedlar, Al	EVA	0.28	0.64	7.7	34	20
OC (4)	36	1	Mono	Tedlar, Al	EVA	0.28	0.62	7.1	31	20
OD (2)	34	1	Mono	Glass	EVA	0.28	0.60	6.6	30	21
OE (2)	36	1	Mono	Tedlar	EVA	0.28	0.63	7.5	32	21
OF (1)	36	1	Mono	Glass	EVA	0.28	0.63	7.3	33	21
OG (2)	36	1	Mono	Tedlar	EVA	0.08	0.53	5.3	8	21
OH (2)	36	1	Mono	Glass	EVA	0.08	0.51	5.5	9	21
OI (2)	36	1	Poly	Tedlar	EVA	0.73	0.15	8.6	42	21
OJ (2)	36	1	Mono	Tedlar	EVA	0.28	0.63	6.6	29	21
PA (2)	36	1	Mono	Tedlar, Al	PVB	0.44	0.71	8.9	52	23
QB (2)	66	2	Mono	Tedlar	EVA	0.52	0.72	9.0	64	23
RA (2)	40	1	Poly	Silicone	Silicone	0.41	0.76	6.3	34	22
RB (6)	36	1	Poly	Silicone	Silicone	0.18	0.70	6.9	18	19
SB (2)	40	1	Poly	—	—	0.4	0.84	7.1	34	23
SC (2)	40	1	Poly	Tedlar	EVA	0.4	0.84	10.9	51	19
SD (2)	36	1	Poly	—	EVA	0.46	0.84	10.3	56	19
UD (2)	40	1	Poly	Tedlar	EVA	0.40	0.84	8.8	42	19
V0 (8)	36	1	Mono	Glass	Silicone	0.27	0.58	5.7	28	20
Y0 (8)	36	1	Mono	Tedlar	EVA	0.27	0.66	7.1	31	23
YB (4)	38	1	Mono	Tedlar	EVA	0.29	0.70	8.7	37	19
YC (4)	36	1	Mono	Tedlar	EVA	0.36	0.81	9.3	41	19

materials. The majority of modules underwent different types of module qualification tests prior to the continuous outdoor exposure. Modules are rated from about 8 Wp up to 117 Wp with average value of around 40 Wp. The number of cells varied from 20 to 144 cells connected in a configuration of 1–8 substrings.

The material of choice for the front side for all types, similar to modern designs, is hardened/tempered glass. Similarly to contemporary products ethylene-vinyl acetate (EVA) was the most widely used encapsulant for tested modules—29 types. However, other types of encapsulants were used, such as polyvinyl butyral (PVB) in 14 cases and polysiloxanes (silicone) in 8 cases. In two cases, the information of the material type is missing. Selection of substrate materials was even more diverse. Like contemporary designs polyvinyl fluoride (tedlar) based foils and combination of tedlar and aluminum foil was the most widely used—21 cases. This was followed by glass—17 cases, silicone—5 cases, polyester/aluminum 4 cases, and 1 case of polyethylene. In five cases, the data about the substrate material was not available. Among tested module types, similar numbers of monocrystalline and polycrystalline cells can be found (31 and 22, respectively). Each of the 53 module types was represented by 1–8 modules with an average of about four modules.

The total exposure time for the different module types varies from 19 to 23 years with the average value over 21 years. The cell packaging density (total active cell area/module area ratio) is lower than for contemporary modules especially for those incorporating monocrystalline round cells, with an average value of 0.66 for monocrystalline and 0.77 for the polycrystalline modules. Low packaging density results in relatively low average modules efficiency:

7.6% for monocrystalline and 8% for polycrystalline modules (11.4 and 9.7% cell efficiency, respectively) considerably lower values to contemporary silicon wafer based modules.

MODULES CHARACTERISATION FOLLOWING LONG-TERM OUTDOOR EXPOSURE

Results of the electrical performance tests of an initial batch of 40 modules following long-term outdoor exposed modules at the ESTI site have been already published.^{4,5} Following the initial investigation of the 40 modules a further 10 modules were removed from the outdoor field (in 2004) with the remaining 154 modules (in 2006). The front surfaces of all of the modules were cleaned and electrical performance tests were conducted according to the IEC 60891⁶ and the IEC 60904 series.^{7–13} The modules then underwent a visual inspection and electrical insulation test following the methods described in the IEC 61215 edition 2.² The results of these measurements are presented in the following sections.

Long-term weathering impact on basic electrical parameters

During the performance measurements the basic electrical parameters: P_{MAX} , I_{SC} , and V_{OC} were determined. Results of the maximum power losses for all module series are presented in the Figures 1 and 2 in the form of bar plots. Figure 1 comprises module series exhibiting average power loss greater than 20%. Module series exhibiting smaller average power losses

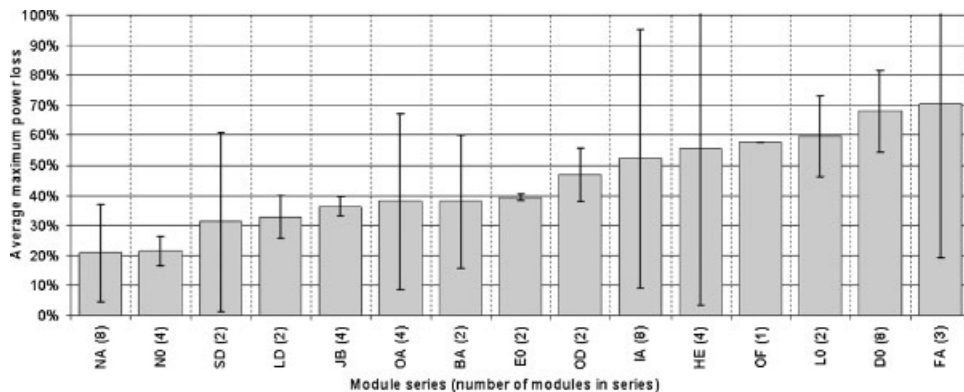


Figure 1. Relative P_{MAX} losses (module types exhibiting average loss greater than 20%)

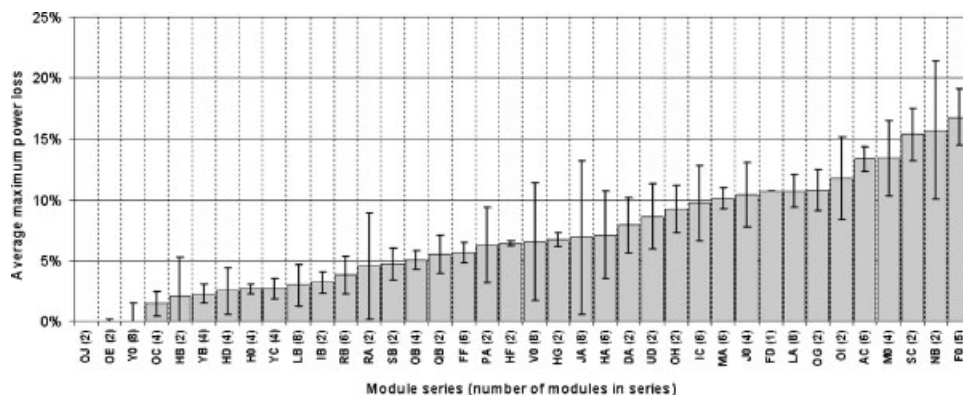


Figure 2. Relative P_{MAX} losses (module types exhibiting average loss smaller than 20%)

are presented in Figure 2. The standard deviations are presented for each series (as dark black lines) giving information on the uniformity of the behavior of each module type (which can be used as an indication of the design and production quality control). The ESTI codes of each series are presented along with the number of modules being tested (in parentheses).

The majority of module series exhibit a very coherent behavior of individual modules. As many as 39 out of the 53 types (74%) exhibit the standard deviation of maximum power change below 5%. This coherent behavior of individual modules within a given module type is true of both modules with small maximum power loss and modules which suffer significant degradation. Seven module series presented in Figure 1 (BA (2), FA (3), HE (4), IA (5), OA (4), SD (2), and NA (8)) out of the 15 types (module series with standard deviation of maximum power change greater than 5%) exhibit significantly higher values of standard deviation greater than 15%. Such a large spread of maximum power losses of modules within one series may indicate serious problems with maintaining quality of the production process.

Some module series comprise modules with total circuit breakage (IA series three modules out of eight failed, HE series two modules out of four, FA series two modules out of three) and therefore exhibit the highest value of standard deviation. The results also indicate some series where very significant power loss or total circuit failure occurred with consistently poor performance of all modules (E0 (2), JB (4), L0 (2), OD (2)), which can indicate low quality of the production process or material quality/design problems.

The mean calculated power loss of all 204 modules is -17.3% with the standard deviation of 23.5% . The power loss is a combination of the losses in the V_{OC} ,

I_{SC} , and FF of the modules. Average losses in other parameters are as follow: I_{SC} : -10.6% , V_{OC} : -5.8% , FF: -9.1% with the standard deviation 18.5, 20, and 22%, respectively. In terms of average loss, V_{OC} reveals the smallest values, with the majority of the module series exhibiting little loss of V_{OC} . The significant losses of V_{OC} exhibited only by six series of modules reflect the loss of one or more substrings of the module. Smaller standard deviation in I_{SC} losses indicate higher uniformity in module behavior but the average I_{SC} loss is almost twice as large as the average loss in V_{OC} .

The I_{SC} and FF are more strongly affected by module aging processes such as, gradual degradation of semiconductor properties, cell interconnections, and also encapsulant browning. The FF loss is usually attributed to an increase of the series resistance due to the degradation of cell interconnections (such as microscopic cracks).¹⁴ One of the non-destructive methods used in the investigation of series resistance is IR imaging of the module under forward bias conditions with short circuit current flow.¹⁵ An example of a thermal image of module NA07 with FF loss of 27.9% can be seen in Figure 3.

The hot spots visible in the images in Figure 3 are places of higher resistance caused by contacts degradation, however, the detection of localized heating by thermal imaging does not always indicate significant FF loss. In some cases, hot spots are caused through cell mismatches.

The comparison of the $I-V$ curves of two modules D002 and NA07 exhibiting significant FF loss is shown in the Figure 4. The curves plotted with the solid line represent measurements performed in the 1980s before long-term outdoor exposure. Dashed lines are the $I-V$

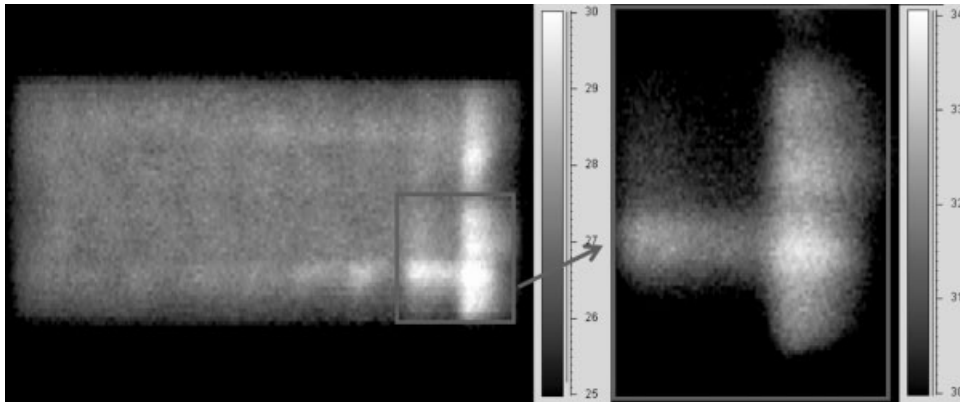


Figure 3. Thermal image of NA07 module under forward bias conditions with short circuit current flow

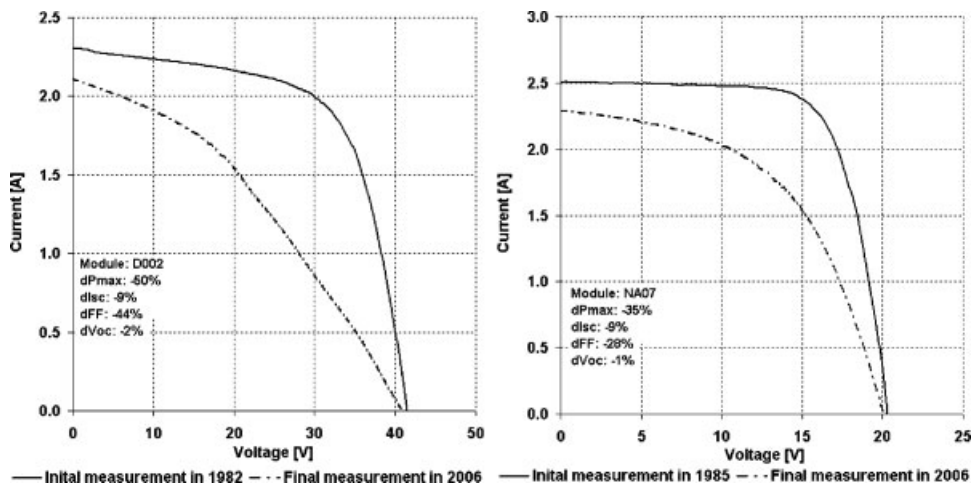


Figure 4. The I - V curves of two modules measured before and after long-term outdoor exposure

curves measured in 2006. It can be observed that both modules lost about 9% of short circuit current due to aging process but main power degradation comes from FF loss (43.7 and 28.9%, respectively).

The scatter plots of the P_{MAX} loss dependence on FF and I_{SC} losses are presented in Figures 5 and 6. It can be observed in Figure 5 that P_{MAX} change is proportional to FF losses especially for high maximum power losses (>20%) which are attributed generally to FF losses (serial resistance increase) with the exception of six modules exhibiting high V_{OC} losses (triangles).

The correlation in I_{SC} and P_{MAX} losses presented in Figure 6 is not so obvious, although some linear correlation is noticeable for moderate modules degradation (I_{SC} losses caused by optical properties degradation

like surface soiling, encapsulant browning, and also light induced doped silicon degradation).^{15,16}

The only module type where high power loss (about 40%, marked with black diamonds in Figures 5 and 6) is correlated to high short circuit loss is the one exhibiting very strong delamination and encapsulant discoloration (Figure 7).

Calculated average annual power degradation

The careful evaluation of an annual performance degradation rate relies on periodic electric characterization of the modules. In the great majority of cases, the modules exposed at Ispra were not periodically checked (some but not representative data exists for individual modules) thus the variation of annual

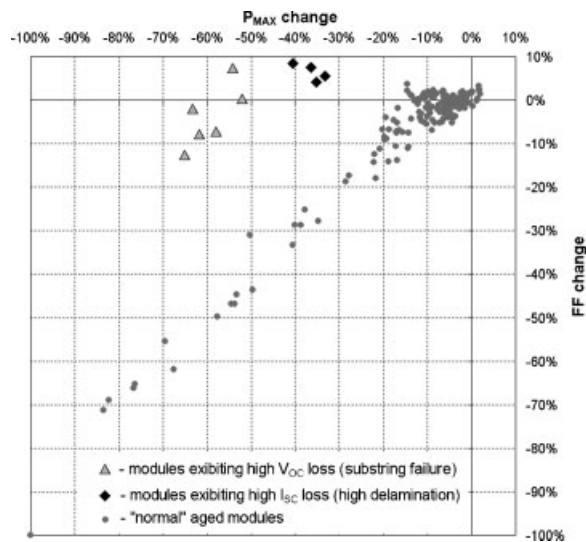


Figure 5. The scatter plot of the dependence of the P_{MAX} losses on the FF losses

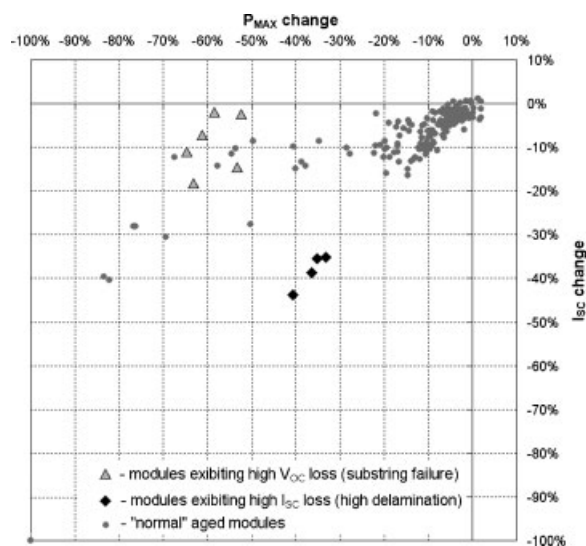


Figure 6. The scatter plot of the dependence of the P_{MAX} losses on the I_{SC} losses

degradation ratio is impossible to obtain. It has been observed by different studies^{5,16} that the degradation rate is faster at the beginning of the exposure (initial degradation) and then stabilizes at a lower level. For long periods of time (the projected lifetime of the photovoltaic plant) an assumption of linear annual degradation rate might be the first approximation for capital investment costs payback time. In this study, the average annual degradation rate was calculated simply by dividing the total degradation rate by the number years of the outdoor exposure. The obtained

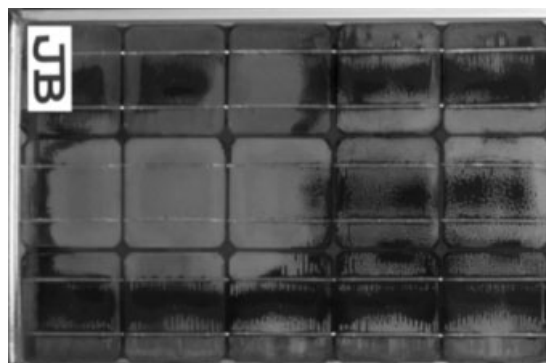


Figure 7. The front surface of the module from JB series exhibiting severe delamination

results are presented in the form of histogram bin plot in Figure 8. More than 70% of modules have annual maximum power degradation rate lower than 0.75%. Modules with the total circuit failure are marked with the black bin. Unfortunately, the failure time for those modules is unknown, but it is obvious that those modules exhibit manufacturing problems resulting in cells interconnections breakage.

Modules preconditioning tests impact on electrical performance

As mentioned previously many modules were subjected to various stress tests (based on the CEC 501 Test Specification) prior to outdoor weathering. In order to identify if there is a systematic relationship between the type of testing sequence and modules performance after long-term exposure, the degradation as a function of test sequence was analysed. The following preconditioning tests were carried out on the modules:

- hot spot heating (HSP); short circuit conditions under $1000 \text{ W/m}^2 \pm 10\%$, 1 h,
- high temperature storage (HTS); $90 \pm 2^\circ\text{C}$, 20 days,
- ultra violet exposure (UVE); $50 \pm 2^\circ\text{C}$, total UV fluence of 15 kWh/m^2 ,
- high temperature high humidity storage (HTH); $90 \pm 2^\circ\text{C}$, $95 \pm 3\%$ RH, 20 days,
- thermal cycling (TC50); from -20 to $+80^\circ\text{C}$, 50 cycles with total duration 400 h,
- humidity freezing (HUF); -20°C , 85% RH, 2 cycles with total duration of 72 h,
- salt mist test (SALT); 35°C , 50 g/L NaCl for 4 days,
- ice formation (ICE); water spraying at -20°C , average ice layer thickness 15 mm,

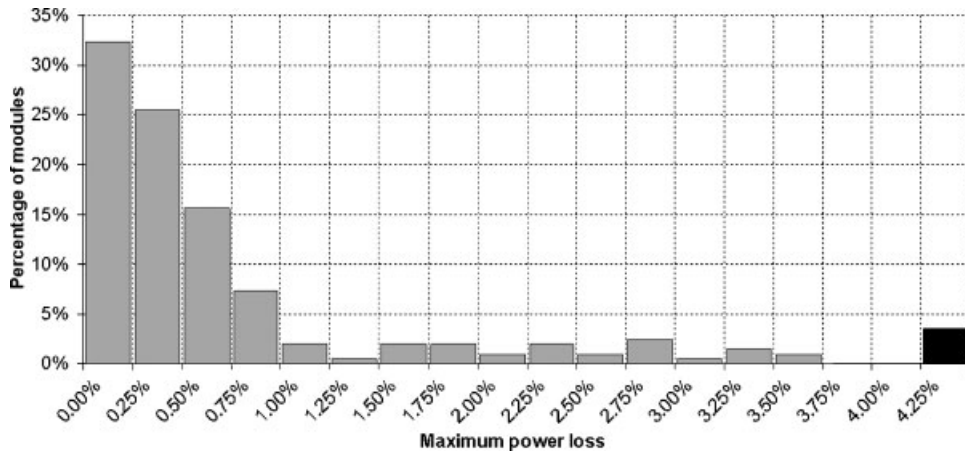


Figure 8. The histogram of average calculated maximum power loss per year

- damp heat (DAH); 85 ± 2°C, 95 ± 3% RH, for 30 days,
- climatic test with O₃ (OZONE); 25°C, 55 ± 3% RH, O₃ concentration 0.5 vpm for 4 days,
- climatic test with SO₂ (SO₂); 40°C, 85% RH, SO₂ concentration 100 vpm for 4 days.

presented results there is no obvious correlation between maximum power loss and initial accelerated stress test.

The impact of the initial accelerated stress tests on later module behavior is difficult to determine since long-term outdoor exposure is the decisive factor in the module electrical performance. Figure 9 shows the maximum power losses of the module series exhibiting the highest values of standard deviation.

There is only one series, HE, in which results can indicate a direct relationship between conditioning test and power loss. Modules HE03 and HE04 exhibit total circuit breakdown while HE01 and HE02 perform fairly well. However, the results can be attributed to different outdoor exposure conditions rather than the type of preconditioning test (HE01 and HE02 were kept at the open circuit while HE03 and HE04 were connected to the maximum power tracker) which will be discussed later in the paper.

Some modules from three series: HE, FA, and IA suffered total circuit breakdown. Modules without prior conditioning are marked with black color. Among the

Concluding, the direct impact of the accelerated stress test was not confirmed but it is to be remembered that the level of the damp heat test and number of thermal cycles was less severe (as shown above) than the levels applied in today's Type Approval Tests.

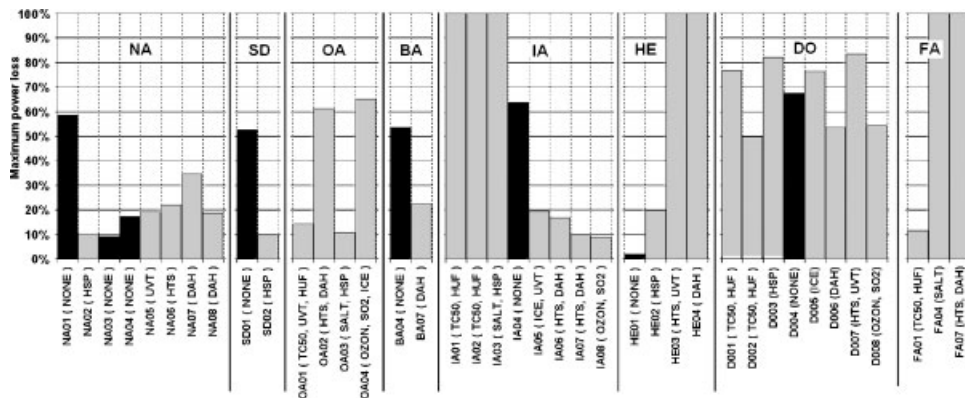


Figure 9. Relative P_{MAX} of selected modules series (black bars—no preconditioning test)

Impact of different encapsulant, back sheet materials, and electrical conditions on modules performance

Module encapsulation ensures protection against weather factors, moisture, oxidation, etc. and provides electrical insulation. The front surface (mostly made of hardened, tempered glass) provides rigidity to withstand mechanical loads, wind, hail, etc. while maintaining high light transmission. The rear non-illuminated layer, mostly made of polymer, polymer/metal foil combination or another glass plate, creates an additional barrier to protect against the weather. Since the investigated modules come from different manufacturers and represent the early generations of PV products, the variety of materials used is significant (described previously).

During long-term outdoor exposure one group of modules was kept at the open circuit conditions (or connected to battery charger used occasionally to charge the batteries of an electric car) while the other group was connected to an inverter with a maximum power point tracker. After about 10 years of exposure all modules were disconnected (due to the outdoor field reorganization) and left in the open circuit conditions.

An influence of different conditions and different materials used for modules construction was investigated with the utilization of statistical method—the analysis of variance (ANOVA). The ANOVA permits to test the statistical significance in which the observed variance (in maximum power loss) is partitioned into components due to different explanatory variables (modules construction details and modules electrical state during long-term outdoor exposure). The results of the variance analysis leads to the conclusion that there is a statistically significant difference between modules groups: the group connected initially to the inverter and modules left in the open circuit conditions (significance $p = 0.00046$) and modules with glass back substrate and polymer one (significance $p = 0.00036$).

The explanation of the results difference regarding electrical conditions during the experiment can be that the current passing through module creates additional thermal stress to cells interconnections (places with higher resistance or mismatched cells). Since interconnection degradation is attributed to changes in solder-joint geometry caused by thermomechanical fatigue (“coarsening”, a change in joint structure, occurs as a result of segregation of the metals, SnPb, in the soldering alloy)¹⁴ elevated temperature due to Joule heating speeds up the interconnections degradation.

There is also difference between groups of modules with the glass back sheet and polymer one. The average value of maximum power loss along with the standard deviation with regard to the modules electrical conditions and the type of the back sheet substrate is presented in Figure 10.

All the modules which exhibit total circuit breakage (seven modules) were connected to the battery charger with maximum power tracking capabilities, while none of modules left in the open circuit conditions suffered total power loss. The calculated (power loss after long-term exposure divided by the exposure time) average annual power degradation for all series is presented in Figure 11. The average annual degradation rate for all connected modules is 1% (0.8% excluding total circuit breakage) and 0.6% for all modules left in the open circuit conditions.

Also, a greater average loss of power was exhibited by glass–glass modules in comparison to glass–polymer modules, however, the spread of the results is very large (there are a lot of cases of modules performing very well while others suffer of total power loss) and the number of investigated modules may not be representative for statistical analysis.

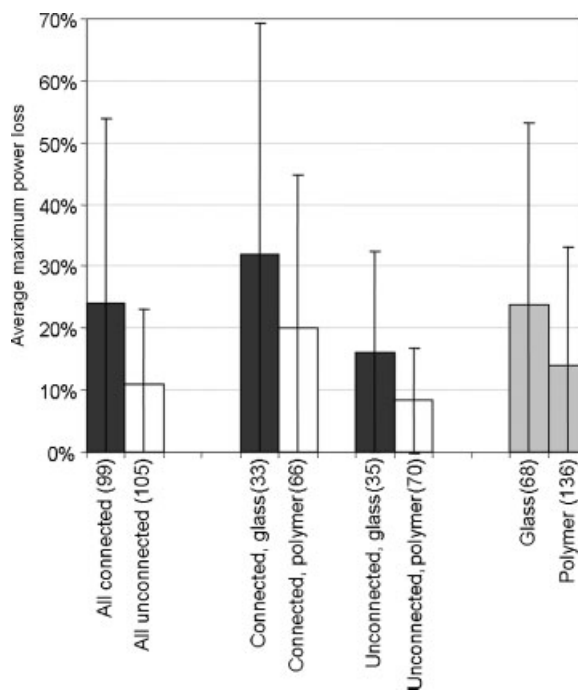


Figure 10. The average value of maximum power loss along with the standard deviation with regard to modules electrical conditions and the type of the substrate material

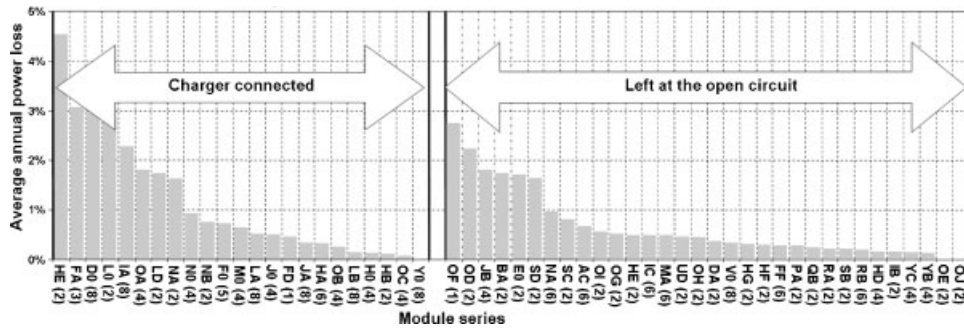


Figure 11. Annual degradation of the maximum power of modules series grouped by module's test conditions

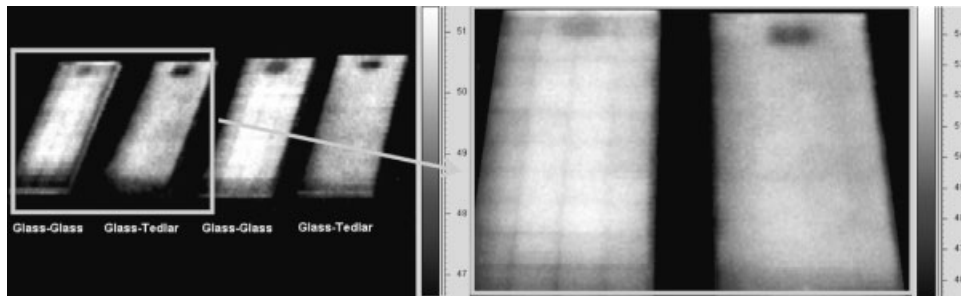


Figure 12. Thermal image of two types of modules under V_{OC} conditions on a sunny, cloudless day

Such a difference may be attributed to different factors. One of the reasons can be related to the different permeability of polymer back sheet material and glass-glass designs to decomposition products of the EVA which trapped within the module package may affect cell interconnections containing aluminum.¹⁷ It was found in Reference¹⁸ that because of the high diffusivity of EVA, even an impermeable glass back sheet alone is incapable of preventing significant moisture ingress from the edges for a 20-year lifecycle.

The difference may also be attributed to the slightly higher cell temperature in the glass-glass modules which causes additional thermomechanical fatigue to the interconnections. The measurement of real cell temperature in a PV module is not a trivial task (requiring thermal sensors encapsulated in the module structure, which is not the case of commercial products), as the recorded temperature at the back of module differs from real cell temperature. Also the determination of the equivalent cell temperature (ECT) by the open circuit method¹⁰ gives an average temperature value, while the temperature within the module is not uniformly distributed.

As an example, four identically sized modules from the same manufacturer, which incorporate the same cell type, encapsulant and frames, differing only in rear

substrate material, were mounted outdoor and the temperature profile was recorded using an Inframetrics 760IR Camera (Figure 12). While the temperature scale is not calibrated to the surface emissivity, the relative measurement indicates temperature difference of magnitude of 2–3°C between the hottest cells of glass-glass modules in comparison to glass-tedlar one. For the other types of modules, however, the real temperature can be different depending on the mounting (stand-alone, façade, or roof integrated), cell type, used encapsulant and how densely the cells are packed.

The performance difference between modules encapsulated with different type of polymer was also investigated (EVA, PVB, or silicone) and the results are shown in Figure 13.

Silicone encapsulated modules exhibit the best performance, however, the reason behind that fact is not clear. The difference may be attributed just to better quality interconnections used by the producers of these modules. Alternatively the improved performance of silicone encapsulated modules over EVA or PVB may be due to better thermomechanical properties. As silicone encapsulants do not require heating to cure,¹⁹ it could be possible that they have a different bonding and thermal expansion to the other EVA or PVB, as such it may place less stress on the cells and

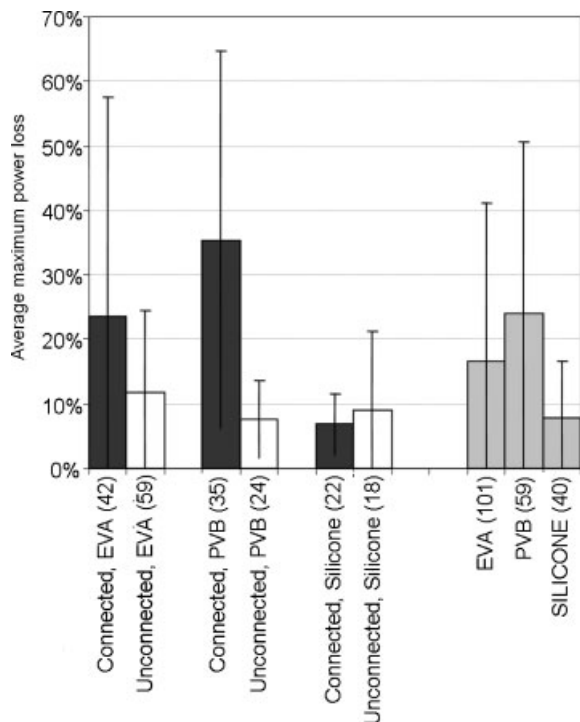


Figure 13. The average value of maximum power loss along with the standard deviation with regard to modules electrical conditions and the type of the encapsulant

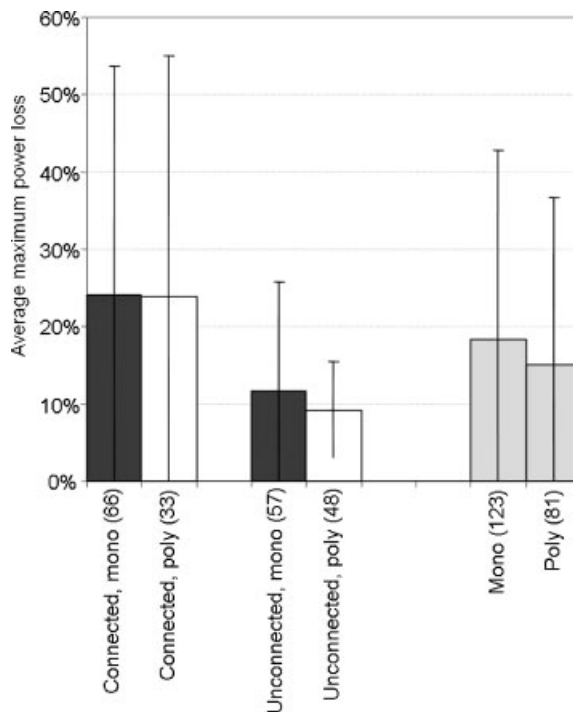


Figure 14. The average value of maximum power loss along with the standard deviation with regard to modules electrical conditions and the cell type

interconnects. However, the spread of results in the power loss demonstrate different production quality issues rather than a systematic difference of modules encapsulated with different types of polymer.

There is no significant statistical difference in the performance of the modules with monocrystalline and polycrystalline cells (Figure 14). This observation is in agreement with data from a study at the National Renewable Energy Laboratory (NREL) which suggest that both monocrystalline and polycrystalline field-aged modules degrade with similar a rate of about 0.7% per year.²⁰ The calculated average annual maximum power degradation depends on the selected samples from the all tested modules. Selecting all monocrystalline and polycrystalline modules including modules exhibiting total circuit breakage due to interconnections failure yielded annual power degradation rates of 0.86 and 0.71%, respectively. Excluding the cases of total circuit failure (series IA, HE, OF exhibiting design problems) the calculated degradation rates are 0.77 and 0.52%. In the case of PV power plant faulty modules might be replaced during maintenance rendering the smaller values of degradation more probable.

The electrical insulation test results

Following the characterization of the electrical performance, the electrical insulation test was performed, according to the recent IEC 61215 edition 2 standard.

This test involves:

- application of a DC voltage of 1000 V plus twice the declared maximum system voltage of the module. If the maximum system voltage does not exceed 50 V, the applied voltage shall be 500 V. Voltage should be maintained at this level for 1 min. Test requirements are met when there is no dielectric breakdown nor surface tracking during the test.
- application of DC voltage 500 V or maximum system voltage of the module, whichever is greater. Voltage should be maintained at this level for 2 min. Test requirements are met when the insulation resistance times the area of the module is greater than 40 M Ω /m² for modules with an area larger than 0.1 m² and 400 M Ω for smaller modules. As the IEC 61215 standard did not exist in the mid 1980s, modules were tested under various voltages levels. To compare the results, the same test levels were applied to modules as had been applied originally. For the

majority of modules (153 modules) the initial insulation test voltage was 1600 V. For 31 modules, a higher initial voltage of 2000 V was applied. The remaining modules were subjected to 1450 V (two modules), 1250 V (four modules), 500 V (eight modules), and 300 V (six modules).

Total failure occurred in six cases (two cases of resistance smaller than $40 \text{ M}\Omega/\text{m}^2$ and four cases of breakdown). In one case, the reason of shorting under applied high voltage was total glass breakage. The other detected problem was caused by the series of modules without junction boxes (connection cables coming directly from the module), in which the junction cables insulation perished causing a short circuit from cable to the module frame.

Surprisingly two modules, which failed during the initial measurement in 1983, passed the insulation test at the same test voltage. No correlation between the insulation resistance and degradation in P_{MAX} or fill factor was observed.

Visual inspection results

The main types of visual defects observed on weathered modules are

- encapsulant browning (cells area and/or the whole module front surface),
- delamination and bubbles formation in the encapsulant,
- back sheet polymer cracks,
- front surface soiling/frosting (ingrained dirt which was not possible to remove),
- blackening at the bottom edge of the module,
- junction box connections corrosion,
- busbar oxidation and discoloration,
- junction cables insulation degradation (modules without junction boxes),
- glass breakage (one case of substrate and one of the front surface).

Usually the observed visual defects are characteristic to the whole module series rather than an individual module and so depict material/production design problems of the whole series. Visual inspection helps to track module design problems but by no means answer the question about module lifetime. There are many examples of optically degraded modules which maintained their original power, while some visually unaffected modules suffered total circuit breakdown. Even modules with totally broken front/back surface

glass can still perform quite well as long as the encapsulant protects from moisture penetration.

CONCLUSIONS

Long-term outdoor exposure is the ultimate test for all module components, material quality and manufacturing quality. More than 20 years of outdoor weathering place the modules encapsulants, cell interconnections, and junction boxes under severe stress. During such time modules received over a $1.5 \text{ MWh}/\text{m}^2$ dose of ultraviolet radiation,²¹ they were subjected to thousands of thermal cycles and thermal stressing in temperatures exceeding 60°C . However, despite the relatively immature module technology from the 1980s, the measured performance after long-term exposure is quite satisfying. The observed results lead to the following conclusions:

- high maximum power losses ($>20\%$) are attributed generally to FF losses (serial resistance increase), while moderate module degradation is caused by I_{SC} loss due to optical properties degradation (change in optical transmittance of the glass and encapsulant) and light induced boron-doped silicon degradation,
- there is no statistically significant difference in the performance of the modules with monocrystalline and polycrystalline cells,
- the maximum power degrades by about 0.8% per year (average value for all tested modules), or by 0.67% (excluding modules with total circuit failure),
- the average annual degradation rate for all modules connected to the battery charger with maximum power capabilities is 1% (0.8% excluding ones exhibiting total circuit breakage) and 0.6% for all modules left in the open circuit conditions,
- there is a statistically significant difference between the group of modules connected initially to the inverter which exhibited approximately twice the degradation in comparison to those modules left in the open circuit conditions,
- there is a difference between groups of modules with a glass–glass construction which show greater degradation than glass–polymer types,
- the visual appearance of field-aged modules is often not correlated with their electrical performance and state of electrical insulation.

Many manufacturers currently give a double power warranty for their products, typically 90% of the initial maximum power after 10 years and 80% of the original maximum power after 25 years. Applying the same

criteria (taking into account modules electrical performance only and assuming 2.5% measurement uncertainty of a testing lab) only 17.6% of modules failed (35 modules out of 204 tested). Remarkably even if we consider the initial warranty period that is 10% of P_{MAX} after 10 years, more than 65.7% of modules exposed for 20 years exceed this criteria. The definition of lifetime is a difficult task as there does not yet appear to be a fixed catastrophic failure point in module ageing but more of a gradual degradation. Therefore, if a system continues to produce energy which satisfies the user need it has not yet reached its end of life. If we consider this level arbitrarily to be the 80% of initial power then all indications from the measurements and observations made in this paper are that the useful lifetime of solar modules is not limited to the commonly assumed 20 years.

REFERENCES

- IEC 61215. *Crystalline Silicon Terrestrial Photovoltaic Modules—Design Qualification and Type Approval*. IEC Central Office: Geneva, Switzerland, 1993.
- IEC 61215. *Crystalline Silicon Terrestrial Photovoltaic Modules—Design Qualification and Type Approval* (2nd edn). IEC Central Office: Geneva, Switzerland, 2005.
- European Commission. *CEC-Specification No. 501, EUR Report 7545 EN*, 1981.
- Dunlop ED, Halton D. The performance of crystalline silicon photovoltaic solar modules after 22 years of continuous outdoor exposure. *Progress in Photovoltaics: Research and Applications* 2006; **14**: 53–64.
- Dunlop ED. Lifetime performance of crystalline silicon PV modules. *Proceedings of the 3rd World Conference on Photovoltaic Energy Conversion*, Osaka Japan, 2003; 2927–2930.
- IEC-60891. *Procedures for Temperature and Irradiance Corrections to Measured I-V Characteristics of Crystalline Silicon PV Devices* (1st edn). IEC Central Office: Geneva, Switzerland, 1987.
- IEC-60904-1. *Measurement of Photovoltaic Current-Voltage Characteristics* (2nd edn). IEC Central Office: Geneva, Switzerland, 2006.
- IEC-60904-2. *Requirements for Reference Solar Device* (2nd edn). IEC Central Office: Geneva, Switzerland, 2007.
- IEC-60904-3. *Measurement Principles for Terrestrial Photovoltaic Solar Devices With Reference Spectral Irradiance Data* (2nd edn). IEC Central Office: Geneva, Switzerland, 2008.
- IEC-60904-5. *Determination of the Equivalent Cell Temperature (ECT) of Photovoltaic Devices by the Open-Circuit Voltage Method*. IEC Central Office: Geneva, Switzerland, 1993.
- IEC-60904-7. *Computation of Spectral Mismatch Error Introduced in the Testing of a Photovoltaic Device* (2nd edn). IEC Central Office: Geneva, Switzerland, 1998.
- IEC-60904-8. *Measurement of Spectral Response of a Photovoltaic Device* (2nd edn). IEC Central Office: Geneva, Switzerland, 1998.
- IEC-60904-9. *Solar Simulator Performance Requirements* (2nd edn). IEC Central Office: Geneva, Switzerland, 2007.
- Quintana MA, King DL, McMahon TJ, Osterwald CR. Commonly observed degradation in field-aged photovoltaic modules. *Photovoltaic Specialists Conference, 2002. Conference Record of the Twenty-Ninth IEEE*, 19–24 May 2002; 1436–1439.
- Morita K, Inoune T, Tsuda I, Hishikawa Y. Degradation factor analysis of c-Si PV modules through long-term field exposure test. *Photovoltaic Energy Conversion, 2003. Proceedings of 3rd World Conference on 12–16 May 2003*; Vol. 2, 1948–1951.
- Tang Y, Raghuraman B, Kuitche J, Tamizhmani G, Backus CE, Osterwald CR. An evaluation of 27+ years old photovoltaic modules operated in a hot-desert climatic condition, photovoltaic testing lab., Arizona State Univ., Mesa, AZ. *Photovoltaic Energy Conversion, Conference Record of the 2006 IEEE 4th World Conference*, May 2006; Waikoloa, USA.
- Kempe MD, Jorgensen GJ, Terwilliger KM, McMahon TJ, Kennedy CE, Borek TT. Ethylene-vinyl acetate potential problems for photovoltaic packaging. *Photovoltaic Energy Conversion, Conference Record of the 2006 IEEE 4th World Conference*, May 2006; Waikoloa, USA.
- Kempe MD. Control of moisture ingress into photovoltaic modules. *Conference Record of the Thirty-First IEEE Photovoltaic Specialists Conference—2005*, Coronado Springs Resort, Lake Buena Vista, FL, 3–7 January 2005.
- Overstraeten V, Martens R. *Physic, Technology and Use of Photovoltaics*, Chapter 8. Adam Hilger Ltd.: Bristol, 1986.
- Osterwald CR, Anderberg A, Rummel S, Ottoson L. Degradation analysis of weathered crystalline-silicon PV modules. *29th IEEE PVSC*, 2002.
- Verdehout JA. European satellite-derived UV climatology available for impact studies. *Radiation Protection Dosimetry* 2004; **111**(4): 407–411.